CORTEX 189 (2025) 20–34

Available online at www.sciencedirect.com

ScienceDirect

Journal homepage: www.elsevier.com/locate/cortex

Research Report

Sparks fade with distance: The effect of electric field distribution on global motion perception using different tES techniques

Andrea Pavan [a,b,*], *Filippo Ghin* [b,c], *Adriano Contillo* [d], *Sibel Akyuz* [e] *and Gianluca Campana* [f,g]

[a] *University of Bologna, Department of Psychology, Bologna, Italy*
[b] *University of Lincoln, School of Psychology, Lincoln, United Kingdom*
[c] *Cognitive Neurophysiology, Department of Child and Adolescent Psychiatry, Faculty of Medicine of the TU Dresden, Dresden, Germany*
[d] *Elettra-Sincrotrone Trieste S.C.p.A, Trieste, Italy*
[e] *University of Bergamo, Department of Human and Social Sciences, Bergamo, Italy*
[f] *University of Padova, Department of General Psychology, Padova, Italy*
[g] *Human Inspired Technology Research Centre, University of Padova, Padova, Italy*

ARTICLE INFO

Article history:
Received 25 January 2025
Revised 4 May 2025
Accepted 12 May 2025
Action editor Nicholas Paul Holmes
Published online 28 May 2025

Keywords:
Global motion
Transcranial electrical stimulation
Electric field
Extracephalic montage

ABSTRACT

Previous evidence has shown that high-frequency transcranial random noise stimulation (hf-tRNS) reduces motion coherence thresholds when applied with a cephalic montage (i.e., return electrode over Cz). Extracephalic montages, which avoid stimulating regions under the return electrode, have also been used to modulate behavioral performance. In this study, we investigated the effects of different transcranial electrical stimulation (tES) protocols on visual motion discrimination, placing the return electrode on the ipsilateral arm. We assessed the impact of electrode positioning using hf-tRNS, anodal, cathodal transcranial direct current stimulation (tDCS), and Sham stimulation over hMT+, a brain region involved in global motion perception. Motion direction discrimination was measured using random dot kinematograms (RDKs). Given the increased distance between the stimulation and return electrodes in this montage, we expected a smaller reduction in motion discrimination thresholds compared to our previous study. Our results suggest that increasing interelectrode distance alters current flow characteristics - such as current distribution and focality - within the cortical areas under the target electrode, producing different effects. Additionally, no significant effects were observed with the other tES protocols tested. Our findings suggest that change in the interelectrode distance influences current flow characteristics, such as current distribution and focality, within the cortical areas under the target electrode, resulting in differential neuromodulatory effects. These results highlight the importance of stimulation configuration on performance, particularly a potential electric field shift due to the change in the interelectrode distance. Given the widespread application of brain stimulation techniques in clinical and cognitive research,

* *Corresponding author*. University of Bologna, Department of Psychology, Viale Berti Pichat, 5, 40127, Bologna, Italy.
E-mail address: andrea.pavan2@unibo.it (A. Pavan).
https://doi.org/10.1016/j.cortex.2025.05.006

our results can guide future studies carefully considering this further aspect of stimulation montage configurations.

1. Introduction

In conventional electrical stimulation, both return and stimulation electrodes are placed on the scalp in different locations to alter cortical excitability within the reach of the electrical field generated by the current flow. Applying an electric field to a neuron induces a change in the resting membrane potential, allowing an electric current to penetrate the membrane, which causes the cell to hyperpolarize or depolarize. This change in the membrane potential may reach the neuron's threshold, triggering neuronal firing (Ye & Steiger, 2015). Modulating neuronal population activity offers a promising approach to altering cortical excitability. The neuromodulatory effects of non-invasive techniques such as transcranial direct current stimulation (tDCS) – in which a weak direct current is applied to the scalp (Stagg & Nitsche, 2011) - and, more recently, transcranial random noise stimulation (tRNS), wherein sinusoidal current alternates between two electrodes across a frequency spectrum (Antal et al., 2008; Terney et al., 2008), have been intensively investigated in the last two decades (Antal et al., 2022; Lefaucheur et al., 2017). More importantly, due to the low incidence of reported adverse effects, non-invasive brain stimulation techniques have been widely applied in both experimental and clinical settings. Although tDCS and transcranial alternating current stimulation (tACS) generally show improvements in clinical contexts, the reported outcomes remain heterogeneous (for reviews, see Berryhill & Martin, 2018; Elyamany et al., 2021).

Random noise stimulation delivers current within a specific band of random frequencies - typically 0–100 Hz for low-frequency tRNS (lf-tRNS) and 101–640 Hz for high-frequency tRNS (hf-tRNS) - to alter cortical excitability. hf-tRNS has been shown to induce long-lasting corticospinal excitability when applied to M1 (Terney et al., 2008; Potok et al., 2021; van der Groen et al., 2022). Cortical modulation via tRNS has also been associated with improvements in motion direction discrimination (Ghin et al., 2018), detection of subthreshold stimuli (van der Groen & Wenderoth, 2016), visual acuity (Moret et al., 2018), perceptual learning (Contemori et al., 2019; Fertonani et al., 2011; Herpich et al., 2015), and working memory (Murphy et al., 2020). Modulatory effects of tRNS have also been reported in attenuating the motion aftereffect (MAE) (Campana et al., 2016). On the other hand, several tRNS studies have reported no-to-mild effects (Mulquiney et al., 2011), and its efficacy in clinical settings remains limited (Battaglini et al., 2019; Brauer et al., 2018; Brevet-Aeby et al., 2019; Nikolin et al., 2020). Despite the evidence suggesting potential benefits of tRNS for some neurological and psychiatric conditions, more systematic evidence and controlled studies are still needed (Herrera-Murillo et al., 2022).

Electric field distribution has been of interest to researchers to characterize how current is conducted through brain tissue, which anatomically includes idiosyncratic components such as skin, skull, fibers, gyral folding, and cerebrospinal fluid (CSF) - all of which affect electrical current flow (Asan et al., 2019; Grant & Lowery, 2009; Opitz et al., 2011). The electric field can also modulate other brain areas along the current trajectory and around the reference electrode, depending on the montage used (Opitz et al., 2016; Parazzini et al., 2011). Studies employing different electrode placements for electrical stimulation have produced somewhat contradictory results. For instance, Moliadze et al. (2010) observed changes in motor-evoked potentials (MEPs) with increasing return electrode distance when using a-tDCS and tRNS. At 1 mA stimulation, increased cortical excitability was observed only with cranial stimulation; however, raising the amplitude to 2 mA induced excitability in both cranial and extracranial configurations. In other words, the loss of excitability due to increased electrode distance was compensated by higher stimulation intensity. Nonetheless, when the distance was further increased, a loss of cortical excitability was again observed.

Additionally, repetitive tDCS with an extracephalic electrode configuration has shown greater improvements in major depressive disorder compared to a bifrontal configuration (Martin et al., 2011). In a simulation study using the Finite Element Method (FEM), Noetscher et al. (2014) suggested that extracephalic montage might increase total current densities in white matter, induce larger average vertical current densities in the primary motor cortex and somatosensory cortex, and result in no change or smaller averages in horizontal current densities for specific cortical areas compared to a cephalic montage. Furthermore, it has been shown that c-tDCS with an extracephalic return electrode arrangement impairs cognitive inhibition (Friehs & Frings, 2019). Accornero et al. (2007) measured visual evoked potentials (VEPs) using tDCS, placing the return electrode at the base of the neck. They reported decreased VEPs with a-tDCS, while c-tDCS led to an increased amplitude of the P1 component.

Fertonani et al. (2011) tested visual perceptual learning performance using different stimulation types - such as a-tDCS, c-tDCS, low- or high-frequency tRNS (hf-tRNS), and Sham stimulation - to investigate their potential effects on behavioral performance. The stimulation electrode was placed over V1, while the return electrode was positioned extracephalically on the right arm. Among all stimulation types, hf-tRNS yielded the most significant improvements in visual perceptual learning. Using an extracephalic electrode and targeting the ventromedial prefrontal cortex (VMPFC) with c-tDCS, Yin et al. (2021) showed that the self-prioritization effect was abolished. In another study,

somewhat mixed results were observed in children with ADHD: no improvements in working memory, cognitive flexibility, or response inhibition were found with either a-tDCS or c-tDCS, whereas only unilateral a-tDCS over the dorsolateral prefrontal cortex (DLPFC) produced partial improvements in executive control (Salehinejad et al., 2022). Both a-tDCS and c-tDCS led to improved accuracy and reaction time in executive function tasks, while decreased working memory performance was observed with c-tDCS in active-duty soldiers (Duffy et al., 2024).

In sum, contradictory results have been shown regarding the efficacy of transcranial electrical stimulation (tES), with some studies highlighting a lack of robust effects on several neurophysiological measures (Horvath et al., 2015a; Horvath et al., 2015b), prompting ongoing debate on the reliability of tES findings (Antal et al., 2015; Horvath et al., 2015a; Price & Hamilton, 2015). Critically, factors such as experimental setup, behavioral paradigms, stimulation intensity, electrode placement, and interindividual variability must be taken into consideration (Fertonani et al., 2017; Horvath et al., 2014; Rodella et al., 2021). Electrode configuration has been suggested as one of the key contributors to these inconsistencies. To our knowledge, no investigation has directly compared the efficacy of cephalic versus extracephalic electrode placements using a motion discrimination paradigm while also examining the effects of different stimulation techniques, such as a-tDCS, c-tDCS, and hf-tRNS. In the present study, we aimed to address design-related disparities in the literature by combining different stimulation types and electrode configurations within the same behavioral paradigm, thereby providing more integrated findings.

Ghin et al. (2018) employed a motion coherence discrimination task using anodal or cathodal tDCS, hf-tRNS, or Sham stimulation. They used a cephalic electrode montage, placing the active electrode over the left hMT+ and the return electrode over the vertex (corresponding to the Cz electrode in a 64-channel EEG system). They found reduced motion coherence thresholds only when the stimulus was presented in the visual hemifield contralateral to the stimulated hMT+. In this study, we investigated the effects of tDCS and hf-tRNS on motion discrimination performance, with particular emphasis on electrode configuration (i.e., cephalic versus extracephalic electrode placement, thereby varying the distance between electrodes) across different brain stimulation types. We expected diminished effects of tES as the distance between the stimulation and return electrodes increased, as suggested by Moliadze et al. (2010) and Opitz et al. (2016). Therefore, the motion coherence threshold reduction induced by hf-tRNS with a cephalic montage, as shown in Ghin et al. (2018), should be reduced or abolished with an extracephalic arrangement. This could be due to a shift in the location of the peak electric field and/or a change in the distribution (focality) of the electric field resulting from increased interelectrode distance. Furthermore, we asked whether other tES types might have any effect on motion coherence thresholds using the same extracephalic arrangement.

In the current investigation, we compared the data from the cephalic stimulation condition in Ghin et al. (2018) with a new dataset using extracephalic stimulation to explore the impact of increased electrode distance on the estimated current field distribution and the resulting behavioral outcomes.

2. Methods

The methods used in this experiment were adapted from Ghin et al. (2018). The paradigm employed in their first experiment was implemented to investigate the effects of increased distance between electrodes.

2.1. Participants

One of the authors (AP) and twelve naïve participants took part in the experiment. All participants had normal or corrected-to-normal vision. All experimental protocols and procedures were conducted in accordance with the World Medical Association (2013) and were approved by the Ethics Committee of the University of Lincoln. Participants were screened using a questionnaire for the presence of implanted metal objects and any past or present history of seizures, heart-related problems, or any neurological conditions, to ensure eligibility for participation. They received detailed information about the protocol and signed a consent form. Participants were given monetary compensation for taking part in the experiment. The cephalic montage dataset used in this study was the same as that reported by Ghin et al. (2018). In contrast, the twelve additional participants in the current study were tested using an extracephalic electrode montage. This approach enabled us to compare the previously reported cephalic stimulation data with the new dataset to evaluate how increased electrode distance influences the estimated current field distribution and the resulting behavioral outcomes.

A post hoc power analysis was conducted using G*Power 3.1 (Faul et al., 2007, 2009) to determine the achieved statistical power for the significant three-way interaction between stimulation type, visual hemifield, and experimental group observed in our mixed ANOVA ($\eta_p^2 = .10$), equivalent to Cohen's $f = .3516$). The analysis was based on a mixed repeated-measures design with eight within-subject measurements (4 stimulation types $\times$ 2 hemifields) and two between-subjects groups (cephalic versus extracephalic montage). The total sample size was 28 participants; one participant (RD) who took part in both experiments was included only once to preserve the independence of observations. With an α level of .05 and non-sphericity correction $\varepsilon = 1$, the power analysis yielded an estimated power of .92, indicating that our sample size was sufficient to detect medium-to-large effects for this interaction.

2.2. Apparatus

Stimuli were presented on a 20-inch HPp1230 monitor with a refresh rate set to 85 Hz. The screen resolution was 1280 $\times$ 1024 pixels, with each pixel corresponding to 1.6 arcmins. The minimum and maximum luminance values of the screen were .08 and 74.6 cd/m^2 respectively, with a mean luminance of 37.5 cd/m^2. Stimuli were displayed on a gamma-

corrected monitor using a look-up table (LUT) to linearize the luminance range. MATLAB Psychtoolbox-3 was used for stimulus generation and data collection (Brainard, 1997; Kleiner et al., 2007; Pelli, 1997). Participants were seated at a 57 cm distance from the screen using a chin and forehead rest.

2.3. Stimuli

Stimuli were random dot kinematograms (RDKs) consisting of 150 randomly moving white dots (.12 deg diameter). RDKs were presented within a circular aperture with a diameter of 8 deg (density: 3 dots/deg^2). Dot drifting speed was 13.4 deg/s, and the eccentricity was 12 deg. However, for four participants the task at 13.4 deg/s was too difficult (occasionally producing the perception of motion in the opposite direction; Bae & Luck, 2022). For these participants only, we used a speed of 8 deg/s. Each dot had a limited lifetime of 47 msec before disappearing and reappearing at another random location within the aperture. Dot density was maintained by repositioning dots that moved outside the circular window. A proportion of the dots moved in a coherent direction (signal dots), while the remaining moved in random directions (noise dots). The probability of a dot being a signal or noise dot was kept constant, and dot appearance on the screen was asynchronous (Geisler, 1999; Morgan & Ward, 1980; Newsome & Paré, 1988). RDKs were displayed for approximately 106 msec and appeared either on the right or left side of the fixation point, randomly selected and counterbalanced.

2.4. Procedure

Participants were instructed to maintain fixation on a central red dot and report the perceived direction of motion of random dot kinematograms (RDKs), presented either in the left or right visual hemifield at an eccentricity of 12° (see Fig. 1 in Ghin et al. (2018) for a schematic representation). The RDKs could move in one of eight possible cardinal or intercardinal directions, and participants responded using an eight-alternative forced choice (8-AFC) task by pressing the corresponding key on the numeric keypad. The 8-AFC task reduces the probability of correct guesses (chance level = 12.5%) and enhances discriminative power relative to simpler alternatives (e.g., 2-AFC). Increasing the number of alternatives improves psychometric efficiency, particularly with adaptive thresholding methods (Hou et al., 2015), and enhances reliability in naïve participants, likely due to greater attentional demands (Jäkel & Wichmann, 2006). Accordingly, the 8-AFC design in our study allowed for a more sensitive detection of tES-induced modulations in motion perception.

Each experimental session began with a brief familiarization phase (no stimulation) to allow participants to become accustomed to the task and response mapping. During this phase, participants completed two blocks of 64 trials each. Within each block, stimuli were presented at 100% coherence, with 32 trials randomly presented in the left visual hemifield and 32 in the right, intermixed in random order. No staircase procedure was used during this phase. Data from the familiarization blocks were not included in the final analyses of coherence thresholds and psychometric function slopes.

Each trial began with the presentation of a fixation point for 1 sec, followed by a brief RDK stimulus. Participants reported the perceived motion direction by pressing one of eight keys on the numeric keypad. No feedback was provided.

Following familiarization, participants completed the main experimental task, which consisted of five consecutive blocks during which transcranial electrical stimulation (tES) was applied. Each block included two interleaved adaptive staircases using the Maximum Likelihood Procedure (MLP; Grassi & Soranzo, 2009; Green, 1993), one tracking the motion coherence threshold for the left visual hemifield, and one for the right. Each staircase consisted of 32 trials. From each staircase, we estimated the motion coherence threshold and slope individually, yielding separate values for each block and each hemifield. The coherence threshold was defined as the coherence level corresponding to 70.7% accuracy.

Transcranial electrical stimulation (a-tDCS, c-tDCS, hf-tRNS, and Sham) was delivered online (i.e., during task execution) across four separate, non-consecutive sessions held on different days. The order of stimulation conditions was counterbalanced across participants. Participants were blinded to the stimulation condition in each session.

2.5. Electrical stimulation

A BrainSTIM EMS device (http://www.brainstim.it/index.php?lang=en) was used for electrical stimulation. The stimulation intensity was set at 1.5 mA with a 30-s ramp-up. The stimulation lasted approximately 18 min. Similar stimulation parameters, when applied over hMT+, have been shown to improve visual motion discrimination with both tDCS (Antal et al., 2004; Battaglini et al., 2017; Wu et al., 2022) and tRNS (Ghin et al., 2018; Pavan et al., 2019). For the hf-tRNS condition, alternating current oscillating at random frequencies between 100 and 600 Hz was delivered. The Sham condition involved 30 sec of stimulation at the beginning of the trial, after which no electrical stimulation was delivered during the task (Gandiga et al., 2006). The electrode placed over hMT$^+$ measured 4 × 4 cm (16 cm^2), while the larger electrode (6 × 10 cm, 60 cm^2) was positioned on the upper left arm, following configurations used in previous studies (Camilleri et al., 2014, 2016; Fertonani et al., 2011; Ghin et al., 2018; Moret et al., 2018; O'Hare et al., 2021). Stimulation was conducted within established safety guidelines (Bikson et al., 2016; Poreisz al., 2007). One electrode was placed over hMT+, the area responsible for visual motion processing (Albright, 1984; Newsome & Paré, 1988; Maunsell & Van Essen, 1983; Smith et al., 2006; Tootell et al., 1995), and the other electrode on the ipsilateral deltoid muscle to create an extracephalic configuration (Fertonani et al., 2011). Since the stimulation electrode was positioned over the left hMT+, the left visual field remained ipsilateral to the stimulated area. Consequently, the modulation of motion discrimination thresholds and slope was anticipated to be most pronounced in the contralateral (right) visual hemifield.

The target area was localized in all participants using predetermined coordinates: 3 cm dorsal to inion and 5 cm to the left, for localization of hMT+ (Battelli et al., 2002; Campana et al., 2002, 2006, 2013; Edwards et al., 2017; Laycock et al., 2007; Pascual-Leone et al., 1999; Pavan et al., 2011, 2017;

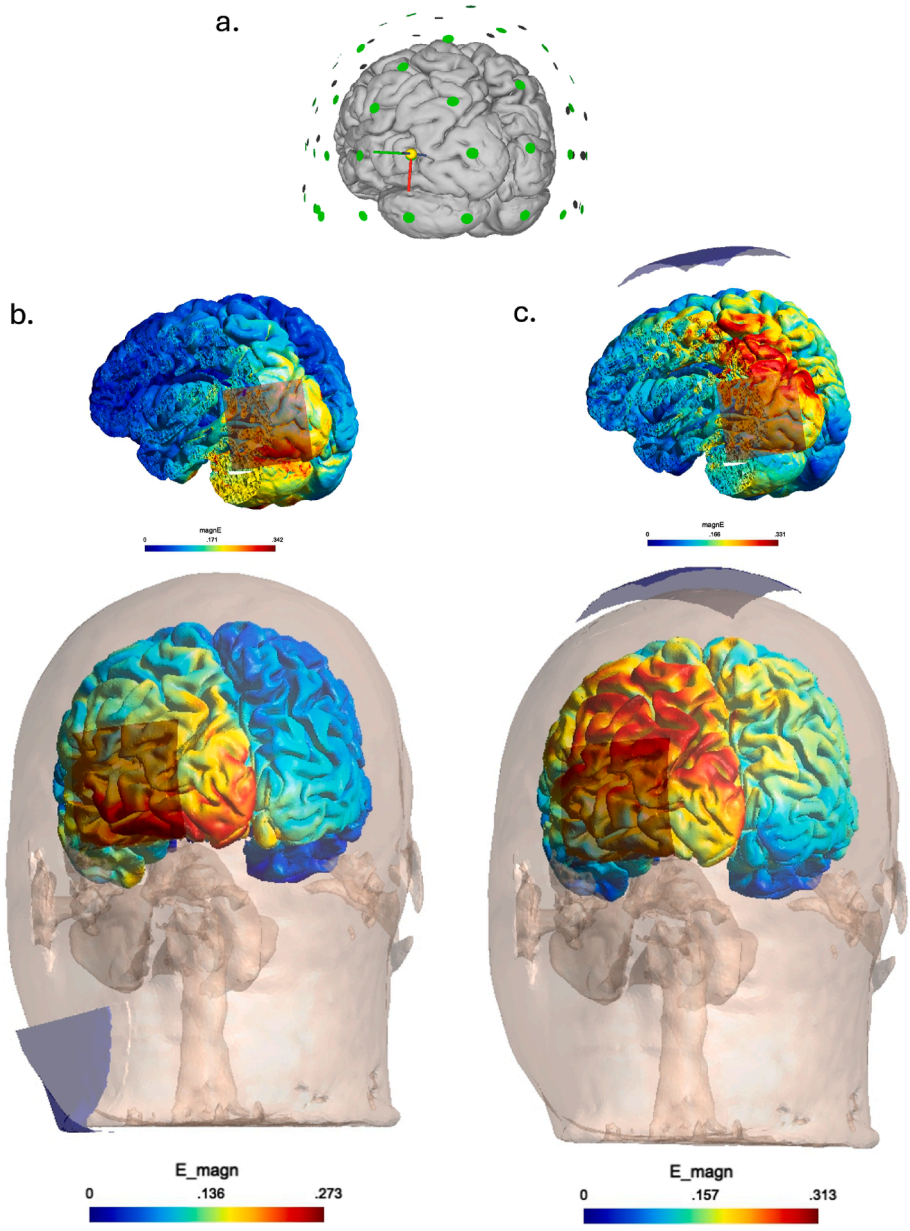

Fig. 1 – Simulated electric field (EF) distribution induced by tES, modeled using SimNIBS. (a) Electrode placement at PO7, corresponding to the left hMT + region, shown in the 10–20 EEG coordinate system. (b) Extracephalic montage using a PO7–neck electrode pair. (c) Cephalic montage using a PO7–Cz electrode pair, following the configuration from Ghin et al. (2018). Color maps represent EF magnitude (E_magn, in V/m), with warmer colors indicating higher field strength.

Théoret et al., 2002). This location aligns with anatomical landmarks (Dumoulin et al., 2000) and functional MRI localizers (Thompson et al., 2009). On an average-sized skull, the closest corresponding electrode position in the 10–20 EEG system is PO7.

2.6. *Estimated electric fields induced by tES*

Simulations were performed using SimNIBS 4.1 (Saturnino et al., 2019; Thielscher et al., 2015) to estimate the potential electric field distribution over hMT+. An extracephalic configuration was employed, with one electrode placed over the area corresponding to hMT+ (as described in the methods section) and the other electrode placed on the ipsilateral neck, given the spatial limitations of the software mesh, which extends to the neck but not the shoulder. Regarding the return location, Maas et al. (2023) showed that electric field (EF) estimates using SimNIBS were largely consistent when comparing lower neck and shoulder return placements. Similarly, Van Hoornweder et al. (2024) suggested neck versus shoulder simulations only showed a .011 V/m peak magnitude difference. Electrode sizes and sponge measurements were kept consistent with those used in the verum tDCS stimulation. Both extracephalic and cephalic electrode configurations

were simulated to assess electric field distribution, following the parameters set by Ghin et al. (2018). The simulations revealed that the 99.9th percentile of the electric field for the extracephalic montage was .307 V/m, slightly lower than the .328 V/m observed for the cephalic configuration (Fig. 1). Focality analysis indicated that 75% of the 99.9th percentile field was confined to a volume of $1.15 \cdot 10^4$ mm^3 in the extracephalic montage, compared to $1.45 \cdot 10^4$ mm^3 in the cephalic configuration. These results suggest that while both configurations produce similar peak electric field magnitudes, the cephalic montage results in a slightly larger and more diffuse field distribution, whereas the extracephalic setup generates a more focused field.

To extrapolate these results to the case of alternating current stimulation, we used a convenient approximation that was first proposed in Ghin et al. (2018). Such approximation allows to extrapolate the expected values of the peak electric field magnitude generated by an alternating current stimulus of given intensity, in terms of the electric field generated by a direct current of equal intensity, if the frequency of the stimulus lies below a threshold value that was quantified in Ghin et al. (2018) in the order of kHz.

The idea underlying the approximation is that the electric field E_ω generated by an alternating current stimulus of frequency ω is proportional to the one E_0 generated by a direct current (that is, when $\omega \to 0$) via a scaling factor r defined as:

$$r = \frac{\sqrt{R_\omega^2 + X_\omega^2}}{R_0} \qquad \text{Eq. 1}$$

R and X are the real and imaginary components of the electrical impedance across the path between the two electrodes (the subscripts refer to the ω frequency stimulus and the direct current stimulus, respectively). Therefore, the knowledge of these components allows us to compute E_ω from E_0.

Unfortunately, the impedance values used in Ghin et al. (2018) refer to a shorter, intracephalic path, and we were not able to retrieve from the literature any estimate of these values for the longer path considered in the present study. Nonetheless, if we make the further assumption that the impedance grows linearly with the path length (which is formally true only along a perfectly homogeneous path, but is still an acceptable approximation as long as several yet similar body tissues are crossed), both the numerator and the denominator of Equation (1) are increased by the same (path length-related) factor, resulting in the same ratio r as in the previous case.

Taking all the above considerations into account, it is possible to claim that the peak electric field experienced in the extracephalic montage ranged approximately from .146 V/m at $\omega = 100$ Hz (when r was .476) to .054 V/m at $\omega = 600$ Hz (when r was .177) whereas the cephalic montage ranged approximately from .156 V/m at $\omega = 100$ Hz (when r was .476) to .058 V/m at $\omega = 600$ Hz (when r was .177). It is important to note that these values are based on a series of approximations and should be regarded as estimates serving only the purpose of this consistency check.

2.7. Data analysis

To examine differences in coherence thresholds between subgroups of participants exposed to stimuli at different speeds, we used a permutation ANOVA (10,000 permutations) with global motion speed as the between-subjects factor. Subsequently, data from the two groups (extracephalic and cephalic montage groups) were analyzed using a three-way mixed ANOVA with one between-subjects factor (montage group) and two within-subjects factors (visual hemifield and stimulation type). Post hoc comparisons were corrected with the FDR method ($\alpha = .05$). The normality of residuals was assessed using QQ plots and the Shapiro–Wilk test.

Skewness of the residual distributions was also assessed. Outliers were identified using the boxplot method, with values above Q3 + 1.5 x IQR or below Q1 - 1.5 x IQR considered outliers. Q1 and Q3 refer to the first and third quartile, respectively, and the interquartile range (IQR) is defined as IQR = Q3 - Q1. The study focused on two dependent variables: (1) the coherence thresholds corresponding to 70.7% correct discrimination, and (2) the slope of the psychometric function. Details of the staircase operational workflow and the calculations for determining coherence threshold and psychometric function slope are provided in Appendix A.

Additionally, to assess whether any practice effect occurred over the course of the experiment and may have influenced our main results, we conducted a series of repeated-measures ANOVAs on coherence thresholds across the five staircase blocks within each experimental condition (cephalic versus extracephalic montage × left versus right visual field).

All analyses and visualizations were conducted using MATLAB 2022b, *R* (v4.3.3) (R Core Team, 2023), and *Jamovi* 2.4 (The jamovi project, 2024).

The materials, data, and scripts used in these experiments are available on the Open Science Framework (OSF) at the following link: https://osf.io/tdq3p/

3. Results

3.1. Coherence thresholds

3.1.1. Permutation ANOVA

The permutation ANOVA was performed using the '*perm.anova*' function from the '*RVAideMemoire*' R package (Hervé, 2020). The results showed no significant difference between the two subgroups in the extracephalic montage when using global motion stimuli at different speeds ($F_{1,\ 102} = .0032$, $p = .952$).

3.2. Coherence thresholds

3.2.1. Omnibus three-way mixed ANOVA

Fig. 2 shows the coherence thresholds for each hemifield and stimulation condition, separately for the cephalic and extracephalic montage. From the QQ plots and Shapiro–Wilk tests performed across all conditions, residuals were approximately normally distributed (all $ps > .05$). Skewness values were around 1 or lower across all conditions, indicating minimal deviation from symmetry. The assumption of homogeneity of variances was also met. One outlier was identified using the boxplot method (cephalic montage group, left visual hemifield, c-tDCS, coherence threshold = 68.1), but it was

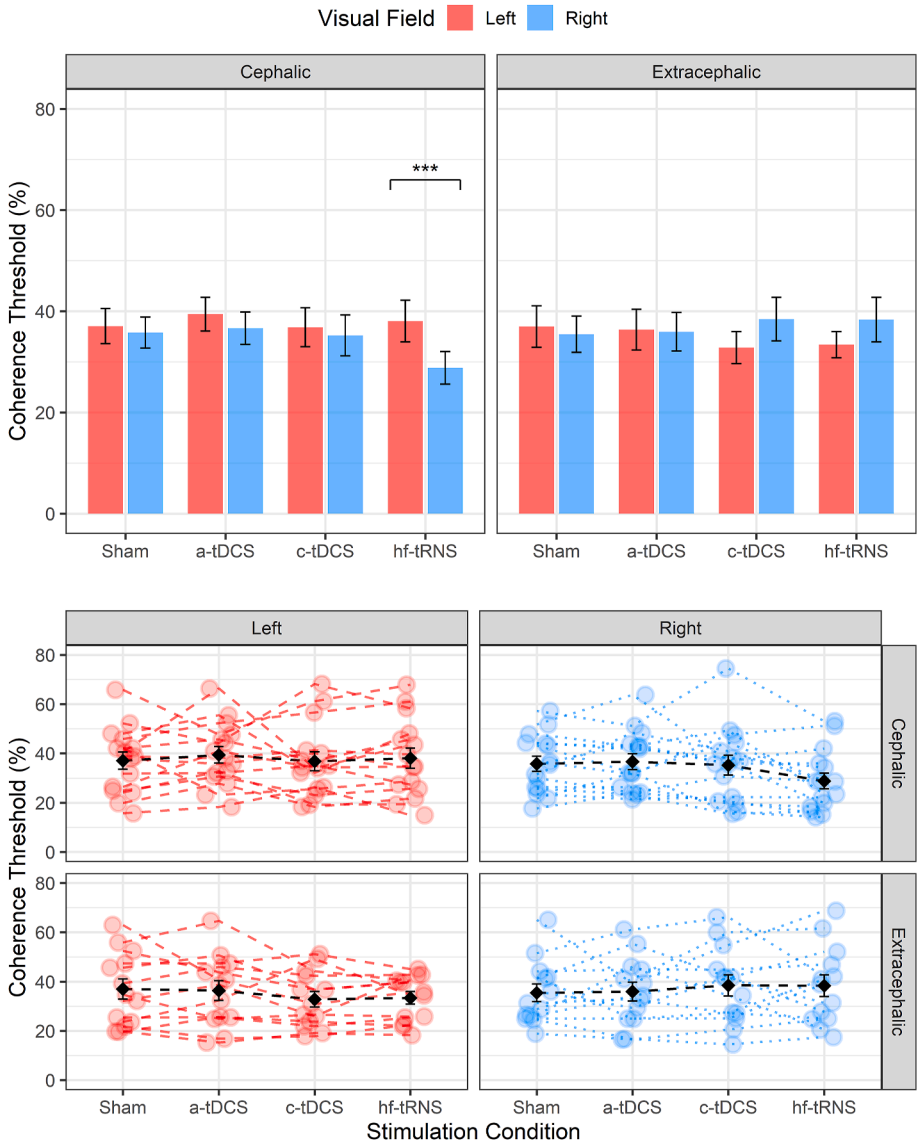

Fig. 2 – Coherence thresholds across stimulation conditions for the cephalic and extracephalic montages. Top panel: Bar plots showing mean coherence thresholds (±1 SEM) for each stimulation condition and visual hemifield, separately for the cephalic and extracephalic groups. Asterisks indicate a significant difference between the left and right visual hemifields in the hf-tRNS condition for the cephalic group ($p_{adj} = .0009$). Bottom panel: Individual data points plotted for each condition and group. Group means are shown as black diamonds with vertical bars indicating ±1 SEM. Black dashed lines connect the group means to facilitate visual comparison across conditions.

retained in the analysis. To further assess this data point, we evaluated its extremeness using a parametric criterion (z-score > ±3) and found that it did not exceed this threshold, indicating it was not a parametric outlier despite being high.

The omnibus mixed ANOVA revealed a significant interaction between group and visual hemifield ($F_{1, 26} = 7.27$, $p = .012$, $\eta_p^2 = .22$), as well as a significant three-way interaction between group, visual hemifield, and stimulation type ($F_{3, 78} = 3.05$, $p = .034$, $\eta_p^2 = .10$). All the other main effects and interactions were not significant (group/montage: $F_{1, 26} < .001$, $p = .99$, $\eta_p^2 < .001$; visual hemifield: $F_{1, 26} = .52$, $p = .48$, $\eta_p^2 = .02$; stimulation: $F_{3, 78} = .80$, $p = .5$, $\eta_p^2 = .03$; stimulation x group: $F_{3, 78} = .62$, $p = .62$, $\eta_p^2 = .023$; visual hemifield x stimulation: $F_{3, 78} = 1.09$, $p = .36$, $\eta_p^2 = .04$). For the interaction between group and visual hemifield, FDR corrected post hoc comparisons (corrected for six comparisons) did not reveal any significant difference (all $p_{adj} > .05$).

To explore the three-way interaction, we performed two-way repeated-measures ANOVA for each group. Specifically, one two-way RM ANOVA for the extracephalic montage and another for the cephalic montage.

For the extracephalic montage, the two-way RM ANOVA did not reveal any significant main effect or interaction (visual hemifield: $F_{1,\ 12} = 1.85$, $p = .2$, $\eta_p^2 = .134$; stimulation: $F_{3,\ 36} = .024$, $p = .99$, $\eta_p^2 = .002$; visual hemifield x stimulation: $F_{3,\ 36} = 1.51$, $p = .23$, $\eta_p^2 = .11$).

For the cephalic montage, the two-way RM ANOVA revealed a significant effect of the visual hemifield ($F_{1,\ 14} = 6.20$, $p = .026$, $\eta_p^2 = .31$) and a significant interaction between visual hemifield and stimulation ($F_{3,\ 42} = 2.9$, $p = .046$, $\eta_p^2 = .17$). The main effect of stimulation was not significant ($F_{1.83,\ 25.63} = 1.64$, $p = .21$, $\eta_p^2 = .11$, Greenhouse–Geisser correction for the degrees of freedom applied due to sphericity violation). On average, coherence thresholds were lower for the right visual hemifield (mean difference: 3.73%; SE: 1.50%). For the significant visual hemifield × stimulation interaction, FDR-corrected post hoc (correction applied for 28 comparisons) revealed a significant difference between left hemifield a-tDCS and right hemifield hf-tRNS conditions ($p_{adj} = .0448$), between left hemifield c-tDCS and right hemifield hf-tRNS conditions ($p_{adj} = .0009$), between left and right hemifields in the hf-tRNS condition ($p_{adj} = .0009$), with a mean difference of 9.25% (SE: 1.91%). A significant difference was also found between left Sham and right hf-tRNS ($p_{adj} = .0009$) and between right Sham and right hf-tRNS conditions ($p_{adj} = .0448$). All other comparisons did not reach the significance level. These findings suggest that hf-tRNS facilitates global motion discrimination by lowering coherence thresholds in the contralateral visual field, but only with a cephalic montage, i.e., when both electrodes are placed on the scalp (see Fig. 2).

3.3. Slope

Fig. 3 shows the slopes for each hemifield and stimulation condition, separately for the cephalic and extracephalic montage. A permutation ANOVA on the slope showed no significant difference between the two subgroups with different global motion speeds in the extracephalic montage ($F_{1,\ 102} = .943$, $p = .335$).

From the QQ plots and Shapiro–Wilk tests conducted for all the conditions (split by montage group), residuals were approximately normally distributed. However, four conditions showed borderline or significant deviations from normality (cephalic, left visual field, a-tDCS, $p = .049$; cephalic, left visual field, c-tDCS, $p = .003$; cephalic, right visual field, hf-tRNS, $p = .022$; extracephalic, right visual field, hf-tRNS, $p = .003$; cephalic, right visual field, Sham, $p = .018$). Nonetheless, skewness values were always <1, suggesting minimal deviation from symmetry. The assumption of sphericity and homogeneity of variances were met. Eight outliers were identified using the boxplot method and were retained in the analysis. To further assess these data points, we applied a parametric criterion (z-score > ±3) and found that none exceeded this threshold. This indicates that, although relatively high or low within their respective conditions, these values do not qualify as parametric outliers. The omnibus mixed ANOVA revealed only a significant interaction between group and visual hemifield ($F_{1,\ 26} = 5.44$, $p = .028$, $\eta_p^2 = .17$). All other main effects and interactions were not significant (group/montage: $F_{1,\ 26} = 3.48$, $p = .074$, $\eta_p^2 = .12$; visual hemifield: $F_{1,\ 26} = .06$, $p = .81$, $\eta_p^2 = .002$; stimulation: $F_{3,\ 78} = .84$, $p = .48$, $\eta_p^2 = .031$; stimulation x group: $F_{3,\ 78} = .21$, $p = .89$, $\eta_p^2 = .008$; visual hemifield x stimulation: $F_{3,\ 78} = .36$, $p = .79$, $\eta_p^2 = .013$; visual hemifield x stimulation x group: $F_{3,\ 78} = 1.213$, $p = .31$, $\eta_p^2 = .045$). For the group x visual hemifield interaction, FDR-corrected post hoc comparisons (corrected for six comparisons) did not reveal any significant difference (all $p_{adj} > .05$). These results suggest that the tES techniques applied had no effect on the slope, which is related to stimulus discriminability.

3.4. Test of practice effects

To assess the presence of practice effects over the course of the experiment, we conducted a series of repeated-measures ANOVAs on coherence thresholds across the five staircase blocks within each experimental condition (cephalic versus extracephalic montage × left versus right visual field). Across all four stimulation conditions, the main effect of the staircase block was not significant, indicating no systematic improvement or deterioration in performance across blocks. Specifically:

Cephalic LVF: $F_{4,\ 56} = .972$, $p = .430$, $\eta_p^2 = .065$;

Cephalic RVF: Greenhouse-Geisser corrected $F_{2.42,\ 33.89} = .494$, $p = .65$, $\eta_p^2 = .034$;

Extracephalic LVF: Greenhouse-Geisser corrected $F_{1.94,\ 23.26} = 2.01$, $p = .158$, $\eta_p^2 = .143$;

Extracephalic RVF: $F_{4,\ 48} = .392$, $p = .813$, $\eta_p^2 = .032$.

Additionally, polynomial trend analyses revealed no significant linear, quadratic, or cubic trends in any condition (all $p > .05$), suggesting the absence of systematic learning effects over time. The Stimulation condition × Block interaction was also non-significant across all analyses (all $p > .05$), even when applying Greenhouse-Geisser corrections for sphericity violations. These consistent findings across all montages and visual hemifields support the conclusion that the stimulation-related effects observed in our study are not confounded by practice effects, and that performance remained stable across repeated measurements.

4. Discussion

Differences in the literature regarding clinical or cognitive applications of brain stimulation are often linked to parameters such as electrode size, position, stimulation type and intensity, duration, and frequency. The extracephalic configuration is often preferred when targeting deeper regions (Bai et al., 2014; Guidetti et al., 2023; Noetscher et al., 2014) or when avoiding stimulation of additional areas under the return electrode. In this study, we aimed to investigate how increased distance between the two electrodes - as occurs in an extracephalic montage – affects neuromodulation.

Our results showed that extracephalic conditions, in general, did not induce changes in motion coherence thresholds: none of the stimulations type altered performance compared

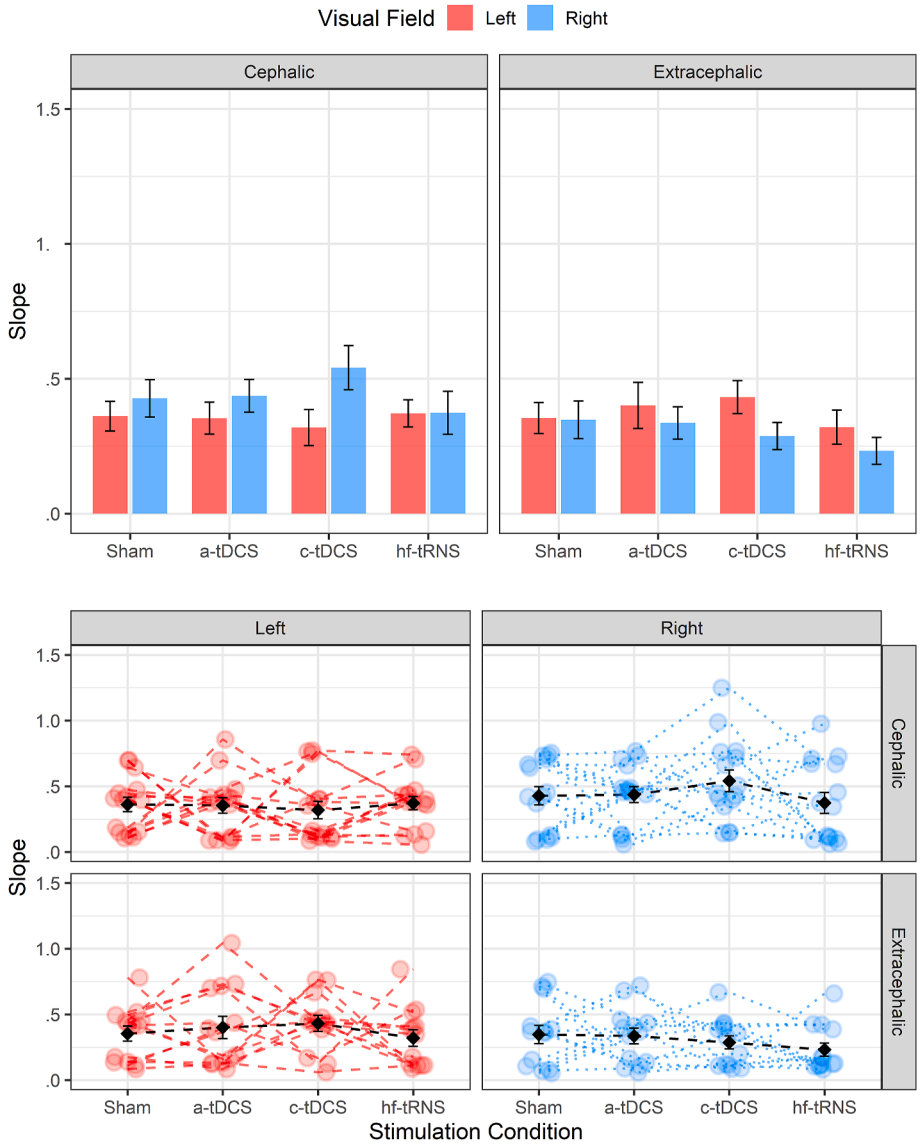

Fig. 3 – Slopes across stimulation conditions for the cephalic and extracephalic montages. Top panel: Bar plots showing mean slopes (±1 SEM) for each stimulation condition and visual hemifield, separately for the cephalic and extracephalic groups. Bottom panel: Individual data points plotted for each condition and group. Group means are shown as black diamonds with vertical bars indicating ±1 SEM. Black dashed lines connect the group means to aid visual comparison across conditions.

to Sham conditions. However, in the cephalic montage, where the interelectrode distance is much smaller, stimulation effects were observed between right and left hemifield conditions. The hf-tRNS condition in the cephalic montage resulted in strong modulations when the globally moving RDK was presented in the visual hemifield contralateral to the stimulation site. Coherence thresholds were lower for the right visual hemifield in the hf-tRNS condition not only compared to the right visual hemifield Sham condition but also compared to the left visual hemifield across the hf-tRNS, a-tDCS, c-tDCS, and Sham conditions. In other words, stimulating over left hMT+ with hf-tRNS overall improved performance (i.e., lowered coherence thresholds) in the motion direction discrimination task when presented in the contralateral hemifield. Neither a-tDCS nor c-tDCS produced significant changes in performance. This may be because online stimulation is optimal for tRNS but sub-optimal for tDCS, whose behavioral effects often require more time to emerge and tend to peak after the stimulation ends (Pirulli et al., 2013). Indeed, both tRNS and tDCS enhance neuronal excitability and performance, but through distinct mechanisms and temporal dynamics. High-frequency tRNS delivers broadband random currents that enhance neural signal processing via a stochastic resonance effect, effectively boosting the signal-to-noise ratio in sensory circuits (Ghin et al., 2018; Pavan et al., 2019; van der Groen & Wenderoth, 2016). In contrast, anodal tDCS applies a low-level constant current that gradually shifts neuronal excitability, resulting in slower, more delayed behavioral

changes. Thus, a key difference lies in the timing of their neuromodulatory effects: tRNS yields immediate benefits during stimulation (online), while tDCS effects typically peak after stimulation has ceased (offline) (Pirulli et al., 2013).

In this study, we run simulations for both cephalic and extracephalic montages to compare the estimated electric field (EF) distributions. Fig. 1 shows the results of increasing interelectrode distance. Traditionally, when a specific region is targeted by electrical stimulation, the stimulation electrode is placed over that area with the expectation of inducing changes in cortical excitability. However, while the cephalic montage estimations appear to target areas responsible for motion perception, such as hMT+, the extracephalic montage seems to shift the EF away from it, towards regions such as the inferior occipital gyrus (IOG), the posterior inferior temporal gyrus (pITG), the temporal pole (TP; not shown in Fig. 1), and the cerebellum. These areas are associated with functions such as face selectivity (IOG; Jacques et al., 2019; de Haas et al., 2021), face recognition and semantic processing (TP; Herlin et al., 2021), object comprehension (anterior temporal lobe; Bonner & Price, 2013), and movement (cerebellum) - none of which directly relate to motion processing. This shift may account for the lack of modulation in coherence thresholds observed across all stimulation types (a-tDCS, c-tDCS, hf-tRNS) in the extracephalic configuration - unlike prior studies that reported behavioral changes using cephalic montages, different stimulation durations, or different stimulation frequency ranges (Antal et al., 2008; Campana et al., 2016; Ghin et al., 2018).

To further explore EF distribution in targeted areas, we conducted SimNIBS simulations of several studies that employed extracephalic montages and reported a lack of behavioral improvements. Salehinejad et al. (2022), who placed the stimulation electrode over the dorsolateral prefrontal cortex (DLFPC), found no improvement in executive function performance using tDCS. Simulation of their stimulation parameters showed higher EF over the ventrolateral prefrontal cortex (VLPFC) rather than the intended DLPFC target (see Supplementary Material Fig. 1 and S1), potentially explaining the absence of behavioral effects. Similarly, Duffy et al. (2024) reported high EF over VLPFC when stimulating the DLPFC. Their results were mixed, with increased reaction time and *d'* for males with a-tDCS and for females with c-tDCS (Fig. S2). Fertonani et al. (2011) found modulation of *d'* with hf-tRNS compared to Sham, a-tDCS, c-tDCS. Simulations of their setup revealed that both occipital lobes were within the peak EF distribution, which is consistent with their reported behavioral effects (Fig. S3). Martin et al. (2011) reported that repeated extracephalic tDCS applied to the DLPFC improved depression scores more than bifrontal stimulation (Drevets, 2007), likely due to widespread EF distribution including limbic areas associated with depressive symptoms (Fig. S4).

In addition to interelectrode distance, electric field (EF) focality plays a critical role in targeting hMT+. Previous studies have shown that focality decreases as interelectrode distance increases in cephalic montages (Caulfield & George, 2022; Mackenbach et al., 2020). Several strategies have been proposed to improve EF focality, such as reducing electrode size (Faria et al., 2011), using ring electrodes (Datta et al., 2009), or increasing the return electrode size (Nitsche et al., 2007). Increasing stimulation intensity could also influence behavioral outcomes, as suggested by Moliadze et al. (2010); however, any intensity manipulation should be carefully considered alongside the estimated spatial distribution of the EF.

Beyond these local targeting concerns, it is also important to consider that the effects of tES are not strictly confined to the targeted cortical site. While our study was not designed to directly assess network-level interactions, we acknowledge that stimulation can influence broader brain networks. This has been clearly demonstrated in several studies combining tES with neuroimaging (e.g., Alekseichuk et al., 2016; Cabral-Calderin et al., 2016; Contò et al., 2021; Kar et al., 2020), which show that stimulation over visual areas, including hMT+, can modulate distributed functional networks involved in motion processing and attention. Although our protocol was optimized for local modulation of hMT+, future studies could benefit from combining tES with EEG or fMRI to directly assess connectivity and network-level dynamics.

This study aimed to present a general overview of how interelectrode distance affects behavioral outcomes through its impact on EF distribution. Based on our simulations, targeting a region of interest under the stimulation electrode appears more precise with a shorter interelectrode distance. In contrast, increasing the distance by moving one electrode to a more distant site may produce unintended effects. Therefore, interelectrode distance should be carefully considered when implementing a tES protocol.

Optimizing tES protocols remains a critical challenge considering its widespread clinical use. The promising outcomes reported in the literature highlight the extensive therapeutic potential of tES. Accordingly, stimulation parameters such as electrode size, interelectrode distance, stimulation type, and intensity must be carefully addressed, and application protocols should be tailored to the specific therapeutic goals.

CRediT authorship contribution statement

Andrea Pavan: Writing – review & editing, Writing – original draft, Supervision, Formal analysis, Conceptualization. **Filippo Ghin:** Writing – review & editing, Writing – original draft, Methodology, Investigation, Data curation. **Adriano Contillo:** Writing – review & editing, Writing – original draft, Visualization, Validation, Data curation. **Sibel Akyuz:** Writing – review & editing, Writing – original draft, Visualization, Software, Formal analysis, Data curation. **Gianluca Campana:** Writing – review & editing, Writing – original draft, Validation, Supervision, Data curation.

Data availability

The materials, data, and scripts used in these experiments are accessible on the Open Science Framework (OSF) at this link: https://osf.io/tdq3p/.

Declaration of competing interest

The authors declare no competing interests.

Acknowledgments

This study was supported by the College of Social Science of the University of Lincoln.

Supplementary data

Supplementary data to this article can be found online at https://doi.org/10.1016/j.cortex.2025.05.006.

Appendix A

Estimation of coherence threshold and slope from MLP

The operational flow of the staircase to estimate coherence threshold and slope of the psychometric function consisted in acquiring and storing the subject response to the n-th trial, selecting the psychometric function maximizing the likelihood of the first n trials, estimating the corresponding coherence threshold, and presenting it as stimulus for the $(n+1)$-th trial. The estimate subsequent to the last trial was the output of the staircase (Grassi & Soranzo, 2009). The logistic function was used as psychometric function:

$$p(x) = \gamma + \frac{1-\gamma}{1+exp(-\beta(x-\alpha))} \quad \text{Eq. (A.1)}$$

The baseline parameter γ was fixed to 1/8, while the midpoint α and the slope parameter β were varied to maximize the likelihood. The rationale for such a choice was to focus on the position of the threshold on the coherence axis, suppressing the further degree of freedom associated with the growth rate of the psychometric function. However, for the sake of completeness, we also extracted information about the slope. To do this, we made use of a custom best fit routine based on a Metropolis–Hastings algorithm, exploring the parameter space of the logistic function. The algorithm randomly selected a starting point in the parameter space $\{\alpha, \beta\}$ and computed the corresponding total likelihood:

$$l_{TOT} = \sum_n ln\left[R_n + (-1)^{R_n} p(x_n)\right] \quad \text{Eq. (A.2)}$$

over the whole staircase. Here x_n is the coherence of the n-th trial, while R_n indicates the corresponding subject response (1 for correct, 0 for wrong). Thereafter, during each iteration of the Metropolis–Hastings, it performed a random step in the parameter space, computed the corresponding total likelihood and compared it to the one of the starting points. If the new likelihood was higher, the algorithm replaced the starting point with the new point, thus accepting the step. Otherwise, the step was rejected. Approximately 100,000 iterations were performed for each staircase, and the logistic function corresponding to the highest likelihood was returned as the best fitting curve. Using the best fit parameters, it was possible to compute an estimate for the coherence threshold T_c as the inverse logistic function:

$$T_c = \alpha - \frac{1}{\beta} ln\left[\frac{1-\gamma}{p_t-\gamma} - 1\right] \quad \text{Eq. (A.3)}$$

p_t being the 70.7% accuracy value acquired by the psychometric function in correspondence of the coherence threshold. The slope of the psychometric function was calculated as:

$$s = \beta\frac{1-\gamma}{4} \quad \text{Eq. (A.4)}$$

where $\gamma = .125$.

Scientific transparency statement

DATA: All raw and processed data supporting this research are publicly available: https://osf.io/tdq3p/.
CODE: All analysis code supporting this research is publicly available: https://osf.io/tdq3p/.
MATERIALS: All study materials supporting this research are publicly available: https://osf.io/tdq3p/.
DESIGN: This article reports, for all studies, how the author(s) determined all sample sizes, all data exclusions, all data inclusion and exclusion criteria, and whether inclusion and exclusion criteria were established prior to data analysis.
PRE-REGISTRATION: No part of the study procedures was pre-registered in a time-stamped, institutional registry prior to the research being conducted. No part of the analysis plans was pre-registered in a time-stamped, institutional registry prior to the research being conducted.
For full details, see the *Scientific Transparency Report* in the supplementary data to the online version of this article.

REFERENCES

Accornero, N., Li Voti, P., La Riccia, M., & Gregori, B. (2007). Visual evoked potentials modulation during direct current cortical polarization. *Experimental Brain Research, 178*(2), 261–266. https://doi.org/10.1007/s00221-006-0733-y

Albright, T. D. (1984). Direction and orientation selectivity of neurons in visual area MT of the macaque. *Journal of Neurophysiology, 52*(6), 1106–1130. https://doi.org/10.1152/jn.1984.52.6.1106

Alekseichuk, I., Turi, Z., Amador de Lara, G., Antal, A., & Paulus, W. (2016). Spatial working memory in humans depends on theta and high gamma synchronization in the prefrontal cortex. *Current Biology, 26*(12), 1513–1521. https://doi.org/10.1016/j.cub.2016.04.035

Antal, A., Boros, K., Poreisz, C., Chaieb, L., Terney, D., & Paulus, W. (2008). Comparatively weak after-effects of transcranial alternating current stimulation (tACS) on cortical excitability in humans. *Brain Stimulation, 1*(2), 97–105.

Antal, A., Keeser, D., Priori, A., Padberg, F., & Nitsche, M. A. (2015). Conceptual and procedural shortcomings of the systematic review "Evidence That Transcranial Direct Current Stimulation (tDCS) Generates Little-to-no Reliable Neurophysiologic Effect Beyond MEP Amplitude Modulation in Healthy Human Subjects: A Systematic Review" by horvath and Co-workers. *Brain Stimulation, 8*(4), 846–849. https://doi.org/10.1016/j.brs.2015.05.010

Antal, A., Kincses, T. Z., Nitsche, M. A., Bartfai, O., & Paulus, W. (2004). Excitability changes induced in the human primary visual cortex by transcranial direct current stimulation: Direct electrophysiological evidence. *Investigative Ophthalmology & Visual Science, 45*(2), 702–707. https://doi.org/10.1167/iovs.03-0688

Antal, A., Luber, B., Brem, A. K., Bikson, M., Brunoni, A. R., Cohen Kadosh, R., Dubljević, V., Fecteau, S., Ferreri, F., Flöel, A., Hallett, M., Hamilton, R. H., Herrmann, C. S., Lavidor, M., Loo, C., Lustenberger, C., Machado, S., Miniussi, C., Moliadze, V., Nitsche, M. A., … Paulus, W. (2022). Non-invasive brain stimulation and neuroenhancement. *Clinical Neurophysiology Practice, 7*, 146–165. https://doi.org/10.1016/j.cnp.2022.05.002

Asan, A. S., Gok, S., & Sahin, M. (2019). Electrical fields induced inside the rat brain with skin, skull, and dural placements of the current injection electrode. *Plos One, 14*(1), Article e0203727. https://doi.org/10.1371/journal.pone.0203727

Bae, G. Y., & Luck, S. J. (2022). Perception of opposite-direction motion in random dot kinematograms. *Visual Cognition, 30*(4), 289–303. https://doi.org/10.1080/13506285.2022.2052216

Bai, S., Dokos, S., Ho, K. A., & Loo, C. (2014). A computational modelling study of transcranial direct current stimulation montages used in depression. *Neuroimage, 87*, 332–344.

Battaglini, L., Contemori, G., Fertonani, A., Miniussi, C., Coccaro, A., & Casco, C. (2019). Excitatory and inhibitory lateral interactions effects on contrast detection are modulated by tRNS. *Scientific Reports, 9*(1), Article 19274. https://doi.org/10.1038/s41598-019-55602-z

Battaglini, L., Noventa, S., & Casco, C. (2017). Anodal and cathodal electrical stimulation over V5 improves motion perception by signal enhancement and noise reduction. *Brain Stimulation, 10*(4), 773–779. https://doi.org/10.1016/j.brs.2017.04.128

Battelli, L., Black, K. R., & Wray, S. H. (2002). Transcranial magnetic stimulation of visual area V5 in migraine. *Neurology, 58*(7), 1066–1069.

Berryhill, M. E., & Martin, D. (2018). Cognitive effects of transcranial direct current stimulation in healthy and clinical populations: An overview. *The Journal of ECT, 34*(3), e25–e35. https://doi.org/10.1097/YCT.0000000000000534

Bikson, M., Grossman, P., Thomas, C., Zannou, A. L., Jiang, J., Adnan, T., Mourdoukoutas, A. P., Kronberg, G., Truong, D., Boggio, P., Brunoni, A. R., Charvet, L., Fregni, F., Fritsch, B., Gillick, B., Hamilton, R. H., Hampstead, B. M., Jankord, R., Kirton, A., Knotkova, H., … Woods, A. J. (2016). Safety of transcranial direct current stimulation: Evidence based update 2016. *Brain Stimulation, 9*(5), 641–661. https://doi.org/10.1016/j.brs.2016.06.004

Bonner, M. F., & Price, A. R. (2013). Where is the anterior temporal lobe and what does it do? *The Journal of Neuroscience, 33*(10), 4213–4215. https://doi.org/10.1523/JNEUROSCI.0041-13.2013

Brainard, D. H., & Vision, S. (1997). The psychophysics toolbox. *Spatial Vision, 10*(4), 433–436.

Brauer, H., Kadish, N. E., Pedersen, A., Siniatchkin, M., & Moliadze, V. (2018). No modulatory effects when stimulating the right inferior frontal gyrus with continuous 6 Hz tACS and tRNS on response inhibition: A behavioral study. *Neural Plasticity, 2018*, Article 3156796. https://doi.org/10.1155/2018/2655073

Brevet-Aeby, C., Mondino, M., Poulet, E., & Brunelin, J. (2019). Three repeated sessions of transcranial random noise stimulation (tRNS) leads to long-term effects on reaction time in the Go/No Go task. *Clinical Neurophysiology, 49*(1), 27–32. https://doi.org/10.1016/j.neucli.2018.10.066

Cabral-Calderin, Y., Anne Weinrich, C., Schmidt-Samoa, C., Poland, E., Dechent, P., Bähr, M., & Wilke, M. (2016). Transcranial alternating current stimulation affects the BOLD signal in a frequency and task-dependent manner. *Human Brain Mapping, 37*(1), 94–121. https://doi.org/10.1002/hbm.23016

Camilleri, R., Pavan, A., & Campana, G. (2016). The application of online transcranial random noise stimulation and perceptual learning in the improvement of visual functions in mild myopia. *Neuropsychologia, 89*, 225–231. https://doi.org/10.1016/j.neuropsychologia.2016.06.024

Camilleri, R., Pavan, A., Ghin, F., Battaglini, L., & Campana, G. (2014). Improvement of uncorrected visual acuity and contrast sensitivity with perceptual learning and transcranial random noise stimulation in individuals with mild myopia. *Frontiers in Psychology, 5*, 1234. https://doi.org/10.3389/fpsyg.2014.01234

Campana, G., Camilleri, R., Moret, B., Ghin, F., & Pavan, A. (2016). Opposite effects of high- and low-frequency transcranial random noise stimulation probed with visual motion adaptation. *Scientific Reports, 6*, Article 38919. https://doi.org/10.1038/srep38919

Campana, G., Cowey, A., & Walsh, V. (2002). Priming of motion direction and area V5/MT: A test of perceptual memory. *Cerebral Cortex (New York, N.Y.: 1991), 12*(6), 663–669. https://doi.org/10.1093/cercor/12.6.663

Campana, G., Cowey, A., & Walsh, V. (2006). Visual area V5/MT remembers "what" but not "where". *Cerebral Cortex (New York, N.Y.: 1991), 16*(12), 1766–1770. https://doi.org/10.1093/cercor/bhj111

Campana, G., Maniglia, M., & Pavan, A. (2013). Common (and multiple) neural substrates for static and dynamic motion after-effects: A rTMS investigation. *Cortex; a Journal Devoted To the Study of the Nervous System and Behavior, 49*(9), 2590–2594. https://doi.org/10.1016/j.cortex.2013.07.001

Caulfield, K. A., & George, M. S. (2022). Optimized APPS-tDCS electrode position, size, and distance doubles the on-target stimulation magnitude in 3000 electric field models. *Scientific Reports, 12*(1), Article 20116. https://doi.org/10.1038/s41598-022-24618-3

Contò, F., Edwards, G., Tyler, S., Parrott, D., Grossman, E., & Battelli, L. (2021). Attention network modulation via tRNS correlates with attention gain. *eLife, 10*, Article e63782. https://doi.org/10.7554/eLife.63782

Contemori, G., Trotter, Y., Cottereau, B. R., & Maniglia, M. (2019). tRNS boosts perceptual learning in peripheral vision. *Neuropsychologia, 125*, 129–136. https://doi.org/10.1016/j.neuropsychologia.2019.02.001

Datta, A., Bansal, V., Diaz, J., Patel, J., Reato, D., & Bikson, M. (2009). Gyri-precise head model of transcranial direct current stimulation: Improved spatial focality using a ring electrode versus conventional rectangular pad. *Brain Stimulation, 2*(4), 201–207.e1. https://doi.org/10.1016/j.brs.2009.03.005

de Haas, B., Sereno, M. I., & Schwarzkopf, D. S. (2021). Inferior occipital gyrus is organized along common gradients of spatial and face-part selectivity. *The Journal of Neuroscience, 41*(25), 5511–5521. https://doi.org/10.1523/JNEUROSCI.2415-20.2021

Drevets, W. C. (2007). Orbitofrontal cortex function and structure in depression. *Annals of the New York Academy of Sciences, 1121*, 499–527. https://doi.org/10.1196/annals.1401.029

Duffy, M. J., Feltman, K. A., Kelley, A. M., & Mackie, R. (2024). Limitations associated with transcranial direct current stimulation for enhancement: Considerations of performance tradeoffs in active-duty soldiers. *Frontiers in Human Neuroscience, 18*, Article 1444450. https://doi.org/10.3389/fnhum.2024.1444450

Dumoulin, S. O., Bittar, R. G., Kabani, N. J., Baker, C. L., Jr., Le Goualher, G., Bruce Pike, G., & Evans, A. C. (2000). A new anatomical landmark for reliable identification of human area V5/MT: A quantitative analysis of sulcal patterning. *Cerebral Cortex, 10*(5), 454–463. https://doi.org/10.1093/cercor/10.5.454

Edwards, G., Paeye, C., Marque, P., VanRullen, R., & Cavanagh, P. (2017). Predictive position computations mediated by parietal areas: TMS evidence. *Neuroimage, 153*, 49–57. https://doi.org/10.1016/j.neuroimage.2017.03.043

Elyamany, O., Leicht, G., Herrmann, C. S., & Mulert, C. (2021). Transcranial alternating current stimulation (tACS): From basic mechanisms towards first applications in psychiatry. *European Archives of Psychiatry and Clinical Neuroscience, 271*(1), 135–156. https://doi.org/10.1007/s00406-020-01209-9

Faria, P., Hallett, M., & Miranda, P. C. (2011). A finite element analysis of the effect of electrode area and inter-electrode distance on the spatial distribution of the current density in tDCS. *Journal of Neural Engineering, 8*(6), Article 066017. https://doi.org/10.1088/1741-2560/8/6/066017

Faul, F., Erdfelder, E., Buchner, A., & Lang, A. G. (2009). Statistical power analyses using G*Power 3.1: Tests for correlation and regression analyses. *Behavior Research Methods, 41*(4), 1149–1160. https://doi.org/10.3758/BRM.41.4.1149

Faul, F., Erdfelder, E., Lang, A. G., & Buchner, A. (2007). G*Power 3: A flexible statistical power analysis program for the social, behavioral, and biomedical sciences. *Behavior Research Methods, 39*(2), 175–191. https://doi.org/10.3758/bf03193146

Fertonani, A., & Miniussi, C. (2017). Transcranial electrical stimulation: What we know and do not know about mechanisms. *The Neuroscientist: a Review Journal Bringing Neurobiology, Neurology and Psychiatry, 23*(2), 109–123. https://doi.org/10.1177/1073858416631966

Fertonani, A., Pirulli, C., & Miniussi, C. (2011). Random noise stimulation improves neuroplasticity in perceptual learning. *The Journal of Neuroscience, 31*(43), 15416–15423. https://doi.org/10.1523/JNEUROSCI.2002-11.2011

Friehs, M. A., & Frings, C. (2019). Cathodal tDCS increases stop-signal reaction time. *Cognitive, Affective & Behavioral Neuroscience, 19*(5), 1129–1142. https://doi.org/10.3758/s13415-019-00740-0

Gandiga, P. C., Hummel, F. C., & Cohen, L. G. (2006). Transcranial DC stimulation (tDCS): A tool for double-blind sham-controlled clinical studies in brain stimulation. *Clinical Neurophysiology, 117*(4), 845–850. https://doi.org/10.1016/j.clinph.2005.12.003

Geisler, W. S. (1999). Motion streaks provide a spatial code for motion direction. *Nature, 400*(6739), 65–69. https://doi.org/10.1038/21886

Ghin, F., Pavan, A., Contillo, A., & Mather, G. (2018). The effects of high-frequency transcranial random noise stimulation (hf-tRNS) on global motion processing: An equivalent noise approach. *Brain Stimulation, 11*(6), 1263–1275. https://doi.org/10.1016/j.brs.2018.07.048

Grant, P. F., & Lowery, M. M. (2009). Electric field distribution in a finite-volume head model of deep brain stimulation. *Medical Engineering & Physics, 31*(9), 1095–1103. https://doi.org/10.1016/j.medengphy.2009.07.006

Grassi, M., & Soranzo, A. (2009). Mlp: A MATLAB toolbox for rapid and reliable auditory threshold estimation. *Behavior Research Methods, 41*(1), 20–28. https://doi.org/10.3758/BRM.41.1.20

Green, D. M. (1993). A maximum-likelihood method for estimating thresholds in a yes-no task. *The Journal of the Acoustical Society of America, 93*(4 Pt 1), 2096–2105. https://doi.org/10.1121/1.406696

Guidetti, M., Maria Bianchi, A., Parazzini, M., Maiorana, N., Bonato, M., Ferrara, R., Libelli, G., Montemagno, K., Ferrucci, R., Priori, A., & Bocci, T. (2023). Monopolar tDCS might affect brainstem reflexes: A computational and neurophysiological study. *Clinical Neurophysiology, 155*, 44–54. https://doi.org/10.1016/j.clinph.2023.08.011

Herlin, B., Navarro, V., & Dupont, S. (2021). The temporal pole: From anatomy to function-A literature appraisal. *Journal of Chemical Neuroanatomy, 113*, Article 101925. https://doi.org/10.1016/j.jchemneu.2021.101925

Herpich, F., Melnick, M., Huxlin, K., Tadin, D., Agosta, S., & Battelli, L. (2015). Transcranial random noise stimulation enhances visual learning in healthy adults. *Journal of Vision, 15*(12), 40. https://doi.org/10.1167/15.12.40, 40.

Herrera-Murillo, M. A., Treviño, M., & Manjarrez, E. (2022). Random noise stimulation in the treatment of patients with neurological disorders. *Neural Regeneration Research, 17*(12), 2557–2562. https://doi.org/10.4103/1673-5374.339474

Hervé, M., & Hervé, M. M. (2020). Package 'RVAideMemoire'. See https://CRANR-projectorg/package=RVAideMemoire.

Horvath, J. C., Carter, O., & Forte, J. D. (2014). Transcranial direct current stimulation: Five important issues we aren't discussing (but probably should be). *Frontiers in Systems Neuroscience, 8*, 2. https://doi.org/10.3389/fnsys.2014.00002

Horvath, J. C., Forte, J. D., & Carter, O. (2015a). Evidence that transcranial direct current stimulation (tDCS) generates little-to-no reliable neurophysiologic effect beyond MEP amplitude modulation in healthy human subjects: A systematic review. *Neuropsychologia, 66*, 213–236. https://doi.org/10.1016/j.neuropsychologia.2014.11.021

Horvath, J. C., Forte, J. D., & Carter, O. (2015b). Quantitative review finds no evidence of cognitive effects in healthy populations from single-session transcranial direct current stimulation (tDCS). *Brain Stimulation, 8*(3), 535–550. https://doi.org/10.1016/j.brs.2015.01.400

Hou, F., Lesmes, L., Bex, P., Dorr, M., & Lu, Z. L. (2015). Using 10AFC to further improve the efficiency of the quick CSF method. *Journal of Vision, 15*(9), 2. https://doi.org/10.1167/15.9.2

Jäkel, F., & Wichmann, F. A. (2006). Spatial four-alternative forced-choice method is the preferred psychophysical method for naïve observers. *Journal of Vision, 6*(11), 1307–1322. https://doi.org/10.1167/6.11.13

Jacques, C., Jonas, J., Maillard, L., Colnat-Coulbois, S., Koessler, L., & Rossion, B. (2019). The inferior occipital gyrus is a major cortical source of the face-evoked N170: Evidence from simultaneous scalp and intracerebral human recordings. *Human Brain Mapping, 40*(5), 1403–1418. https://doi.org/10.1002/hbm.24455

Kar, K., Ito, T., Cole, M. W., & Krekelberg, B. (2020). Transcranial alternating current stimulation attenuates BOLD adaptation and increases functional connectivity. *Journal of Neurophysiology, 123*(1), 428–438. https://doi.org/10.1152/jn.00376.2019

Kleiner, M., Brainard, D., & Pelli, D. (2007). *What's new in Psychtoolbox-3? Perception 36 ECVP abstract supplement*.

Laycock, R., Crewther, D. P., Fitzgerald, P. B., & Crewther, S. G. (2007). Evidence for fast signals and later processing in human V1/V2 and V5/MT+: A TMS study of motion perception. *Journal of Neurophysiology, 98*(3), 1253–1262. https://doi.org/10.1152/jn.00416.2007

Lefaucheur, J. P., Antal, A., Ayache, S. S., Benninger, D. H., Brunelin, J., Cogiamanian, F., Cotelli, M., De Ridder, D., Ferrucci, R., Langguth, B., Marangolo, P., Mylius, V., Nitsche, M. A., Padberg, F., Palm, U., Poulet, E., Priori, A., Rossi, S., Schecklmann, M., Vanneste, S., … Paulus, W. (2017). Evidence-based guidelines on the therapeutic use of transcranial direct current stimulation (tDCS). *Clinical Neurophysiology, 128*(1), 56–92. https://doi.org/10.1016/j.clinph.2016.10.087

Maas, R. P. P. W. M., Faber, J., ESMI MR Study Group, van de Warrenburg, B. P. C., & Schutter, D. J. L. G. (2023). Interindividual differences in posterior fossa morphometry affect cerebellar tDCS-induced electric field strength. *Clinical Neurophysiology, 153*, 152–165. https://doi.org/10.1016/j.clinph.2023.06.019

Mackenbach, C., Tian, R., & Yang, Y. (2020). Effects of electrode configurations and injected current intensity on the electrical field of transcranial direct current stimulation: A simulation study. In *Annual International Conference of the IEEE Engineering in Medicine and Biology Society. IEEE Engineering in Medicine and Biology Society. Annual International Conference, 2020* (pp. 3517–3520). https://doi.org/10.1109/EMBC44109.2020.9176686

Martin, D. M., Alonzo, A., Mitchell, P. B., Sachdev, P., Gálvez, V., & Loo, C. K. (2011). Fronto-extracephalic transcranial direct current stimulation as a treatment for major depression: An open-label pilot study. *Journal of Affective Disorders, 134*(1–3), 459–463. https://doi.org/10.1016/j.jad.2011.05.018

Maunsell, J. H., & Van Essen, D. C. (1983). Functional properties of neurons in middle temporal visual area of the macaque monkey. I. Selectivity for stimulus direction, speed, and orientation. *Journal of Neurophysiology, 49*(5), 1127–1147. https://doi.org/10.1152/jn.1983.49.5.1127

Moliadze, V., Antal, A., & Paulus, W. (2010). Electrode-distance dependent after-effects of transcranial direct and random noise stimulation with extracephalic reference electrodes. *Clinical Neurophysiology, 121*(12), 2165–2171. https://doi.org/10.1016/j.clinph.2010.04.033

Moret, B., Camilleri, R., Pavan, A., Lo Giudice, G., Veronese, A., Rizzo, R., & Campana, G. (2018). Differential effects of high-frequency transcranial random noise stimulation (hf-tRNS) on contrast sensitivity and visual acuity when combined with a short perceptual training in adults with amblyopia. *Neuropsychologia, 114*, 125–133. https://doi.org/10.1016/j.neuropsychologia.2018.04.017

Morgan, M. J., & Ward, R. (1980). Interocular delay produces depth in subjectively moving noise patterns. *The Quarterly Journal of Experimental Psychology: QJEP, 32*(3), 387–395. https://doi.org/10.1080/14640748008401833

Mulquiney, P. G., Hoy, K. E., Daskalakis, Z. J., & Fitzgerald, P. B. (2011). Improving working memory: Exploring the effect of transcranial random noise stimulation and transcranial direct current stimulation on the dorsolateral prefrontal cortex. *Clinical Neurophysiology : Official Journal of the International Federation of Clinical Neurophysiology, 122*(12), 2384–2389. https://doi.org/10.1016/j.clinph.2011.05.009

Murphy, O. W., Hoy, K. E., Wong, D., Bailey, N. W., Fitzgerald, P. B., & Segrave, R. A. (2020). Transcranial random noise stimulation is more effective than transcranial direct current stimulation for enhancing working memory in healthy individuals: Behavioural and electrophysiological evidence. *Brain Stimulation, 13*(5), 1370–1380. https://doi.org/10.1016/j.brs.2020.07.001

Newsome, W. T., & Paré, E. B. (1988). A selective impairment of motion perception following lesions of the middle temporal visual area (MT). *The Journal of Neuroscience, 8*(6), 2201–2211. https://doi.org/10.1523/JNEUROSCI.08-06-02201.1988

Nikolin, S., Alonzo, A., Martin, D., Gálvez, V., Buten, S., Taylor, R., Goldstein, J., Oxley, C., Hadzi-Pavlovic, D., & Loo, C. K. (2020). Transcranial random noise stimulation for the acute treatment of depression: A randomized controlled trial. *The International Journal of Neuropsychopharmacology, 23*(3), 146–156. https://doi.org/10.1093/ijnp/pyz072

Nitsche, M. A., Doemkes, S., Karaköse, T., Antal, A., Liebetanz, D., Lang, N., Tergau, F., & Paulus, W. (2007). Shaping the effects of transcranial direct current stimulation of the human motor cortex. *Journal of Neurophysiology, 97*(4), 3109–3117. https://doi.org/10.1152/jn.01312.2006

Noetscher, G. M., Yanamadala, J., Makarov, S. N., & Pascual-Leone, A. (2014). Comparison of cephalic and extracephalic montages for transcranial direct current stimulation–a numerical study. *IEEE Transactions on Bio-medical Engineering, 61*(9), 2488–2498. https://doi.org/10.1109/TBME.2014.2322774

O'Hare, L., Goodwin, P., Sharp, A., Contillo, A., & Pavan, A. (2021). Improvement in visual perception after high-frequency transcranial random noise stimulation (hf-tRNS) in those with migraine: An equivalent noise approach. *Neuropsychologia, 161*, Article 107990. https://doi.org/10.1016/j.neuropsychologia.2021.107990

Opitz, A., Falchier, A., Yan, C. G., Yeagle, E. M., Linn, G. S., Megevand, P., Thielscher, A., Deborah A, R., Milham, M. P., Mehta, A. D., & Schroeder, C. E. (2016). Spatiotemporal structure of intracranial electric fields induced by transcranial electric stimulation in humans and nonhuman primates. *Scientific Reports, 6*, Article 31236. https://doi.org/10.1038/srep31236

Opitz, A., Windhoff, M., Heidemann, R. M., Turner, R., & Thielscher, A. (2011). How the brain tissue shapes the electric field induced by transcranial magnetic stimulation. *Neuroimage, 58*(3), 849–859. https://doi.org/10.1016/j.neuroimage.2011.06.069

Parazzini, M., Fiocchi, S., Rossi, E., Paglialonga, A., & Ravazzani, P. (2011). Transcranial direct current stimulation: Estimation of the electric field and of the current density in an anatomical human head model. *IEEE Transactions on Bio-medical Engineering, 58*(6), 1773–1780. https://doi.org/10.1109/TBME.2011.2116019

Pascual-Leone, A., Tarazona, F., Keenan, J., Tormos, J. M., Hamilton, R., & Catala, M. D. (1999). Transcranial magnetic stimulation and neuroplasticity. *Neuropsychologia, 37*(2), 207–217. https://doi.org/10.1016/s0028-3932(98)00095-5

Pavan, A., Alexander, I., Campana, G., & Cowey, A. (2011). Detection of first- and second-order coherent motion in blindsight. *Experimental Brain Research, 214*(2), 261–271. https://doi.org/10.1007/s00221-011-2828-3

Pavan, A., Ghin, F., Contillo, A., Milesi, C., Campana, G., & Mather, G. (2019). Modulatory mechanisms underlying high-frequency transcranial random noise stimulation (hf-tRNS): A combined stochastic resonance and equivalent noise approach. *Brain Stimulation, 12*(4), 967–977. https://doi.org/10.1016/j.brs.2019.02.018

Pavan, A., Ghin, F., Donato, R., Campana, G., & Mather, G. (2017). The neural basis of form and form-motion integration from static and dynamic translational Glass patterns: A rTMS investigation. *Neuroimage, 157*, 555–560. https://doi.org/10.1016/j.neuroimage.2017.06.036

Pelli, D. G. (1997). The VideoToolbox software for visual psychophysics: Transforming numbers into movies. *Spatial Vision, 10*(4), 437–442.

Pirulli, C., Fertonani, A., & Miniussi, C. (2013). The role of timing in the induction of neuromodulation in perceptual learning by transcranial electric stimulation. *Brain Stimulation, 6*(4), 683–689. https://doi.org/10.1016/j.brs.2012.12.005

Poreisz, C., Boros, K., Antal, A., & Paulus, W. (2007). Safety aspects of transcranial direct current stimulation concerning healthy subjects and patients. *Brain Research Bulletin, 72*(4–6), 208–214. https://doi.org/10.1016/j.brainresbull.2007.01.004

Potok, W., Bächinger, M., van der Groen, O., Cretu, A. L., & Wenderoth, N. (2021). Transcranial random noise stimulation acutely lowers the response threshold of human motor circuits. *The Journal of Neuroscience : the Official Journal of the Society for Neuroscience, 41*(17), 3842–3853. https://doi.org/10.1523/JNEUROSCI.2961-20.2021

Price, A. R., & Hamilton, R. H. (2015). A Re-evaluation of the cognitive effects from single-session transcranial direct current stimulation. *Brain Stimulation, 8*(3), 663–665. https://doi.org/10.1016/j.brs.2015.03.007

Rodella, C., Cespón, J., Repetto, C., & Pellicciari, M. C. (2021). Customized application of tDCS for clinical rehabilitation in Alzheimer's disease. *Frontiers in Human Neuroscience, 15*, Article 687968. https://doi.org/10.3389/fnhum.2021.687968

Salehinejad, M. A., Vosough, Y., & Nejati, V. (2022). The impact of bilateral anodal tDCS over left and right DLPFC on executive functions in children with ADHD. *Brain Sciences, 12*(8), 1098. https://doi.org/10.3390/brainsci12081098

Saturnino, G. B., Puonti, O., Nielsen, J. D., Antonenko, D., Madsen, K. H., & Thielscher, A. (2019). SimNIBS 2.1: A comprehensive pipeline for individualized electric field modelling for transcranial brain stimulation. In S. Makarov, et al. (Eds.), *Brain and human body modeling: Computational human modeling at EMBC 2018* (pp. 3–25). Springer.

Smith, A. T., Wall, M. B., Williams, A. L., & Singh, K. D. (2006). Sensitivity to optic flow in human cortical areas MT and MST. *The European Journal of Neuroscience, 23*(2), 561–569. https://doi.org/10.1111/j.1460-9568.2005.04526.x

Stagg, C. J., & Nitsche, M. A. (2011). Physiological basis of transcranial direct current stimulation. *The Neuroscientist: A Review Journal Bringing Neurobiology, Neurology and Psychiatry, 17*(1), 37–53. https://doi.org/10.1177/1073858410386614

Terney, D., Chaieb, L., Moliadze, V., Antal, A., & Paulus, W. (2008). Increasing human brain excitability by transcranial high-frequency random noise stimulation. *The Journal of Neuroscience, 28*(52), 14147–14155. https://doi.org/10.1523/JNEUROSCI.4248-08.2008

Théoret, H., Kobayashi, M., Ganis, G., Di Capua, P., & Pascual-Leone, A. (2002). Repetitive transcranial magnetic stimulation of human area MT/V5 disrupts perception and storage of the motion aftereffect. *Neuropsychologia, 40*(13), 2280–2287. https://doi.org/10.1016/s0028-3932(02)00112-4

The jamovi project. (2024). *Jamovi (Version 2.4)* [Computer Software]. Retrieved from https://www.jamovi.org.

Thielscher, A., Antunes, A., & Saturnino, G. B. (2015). Field modeling for transcranial magnetic stimulation: A useful tool to understand the physiological effects of TMS?. In *Annual International Conference of the IEEE Engineering in Medicine and Biology Society, IEEE Engineering in Medicine and Biology Society. Annual International Conference, 2015* (pp. 222–225). https://doi.org/10.1109/EMBC.2015.7318340

Thompson, B., Aaen-Stockdale, C., Koski, L., & Hess, R. F. (2009). A double dissociation between striate and extrastriate visual cortex for pattern motion perception revealed using rTMS. *Human Brain Mapping, 30*(10), 3115–3126. https://doi.org/10.1002/hbm.20736

Tootell, R. B., Reppas, J. B., Kwong, K. K., Malach, R., Born, R. T., Brady, T. J., Rosen, B. R., & Belliveau, J. W. (1995). Functional analysis of human MT and related visual cortical areas using magnetic resonance imaging. *The Journal of Neuroscience, 15*(4), 3215–3230. https://doi.org/10.1523/JNEUROSCI.15-04-03215.1995

van der Groen, O., Potok, W., Wenderoth, N., Edwards, G., Mattingley, J. B., & Edwards, D. (2022). Using noise for the better: The effects of transcranial random noise stimulation on the brain and behavior. *Neuroscience and Biobehavioral Reviews, 138*, Article 104702. https://doi.org/10.1016/j.neubiorev.2022.104702

van der Groen, O., & Wenderoth, N. (2016). Transcranial random noise stimulation of visual cortex: Stochastic resonance enhances central mechanisms of perception. *The Journal of Neuroscience, 36*(19), 5289–5298. https://doi.org/10.1523/JNEUROSCI.4519-15.2016

Van Hoornweder, S., Cappozzo, V., De Herde, L., Puonti, O., Siebner, H., Meesen, R., & Thielscher, A. (2024). Head and shoulders-the impact of an extended head model on the simulation and optimization of transcranial electric stimulation. *bioRxiv, 2024–08*.

World Medical Association. (2013). World Medical Association Declaration of Helsinki: ethical principles for medical research involving human subjects. *JAMA, 310*(20), 2191–2194. https://doi.org/10.1001/jama.2013.281053

Wu, D., Wang, Y., Liu, N., Wang, P., Sun, K., & Xiao, W. (2022). High-definition transcranial direct current stimulation of the left middle temporal complex does not affect visual motion perception learning. *Frontiers in Neuroscience, 16*, Article 988590. https://doi.org/10.3389/fnins.2022.988590

Ye, H., & Steiger, A. (2015). Neuron matters: Electric activation of neuronal tissue is dependent on the interaction between the neuron and the electric field. *Journal of Neuroengineering and Rehabilitation, 12*, 65. https://doi.org/10.1186/s12984-015-0061-1

Yin, S., Bi, T., Chen, A., & Egner, T. (2021). Ventromedial prefrontal cortex drives the prioritization of self-associated stimuli in working memory. *Journal of Neuroscience, 41*(9), 2012–2023.